Taylor & Francis
Taylor & Francis Group

ORIGINAL RESEARCH

🔓 OPEN ACCESS | Check for updates

Increased tryptophan, but not increased glucose metabolism, predict resistance of pembrolizumab in stage III/IV melanoma

Jorge D. Oldan[a,b], Benjamin C. Giglio[b], Eric Smith[a,b], Weiling Zhao[b], Deeanna M. Bouchard[c], Marija Ivanovic[a,b], Yueh Z. Lee[a,b], Frances A. Collichio[c,d], Michael O. Meyers[c,i], Diana E. Wallack[c], Amber Abernethy-Leinwand[b], Patricia K. Long[c,i], Dimitri G. Trembath[e], Paul B. Googe[f], Madeline H. Kowalski[g], Anastasia Ivanova[g], Jennifer A. Ezzell[h] Nana Nikolaishvili-Feinberg[c], Nancy E. Thomas[c,f], Terence Z. Wong[a,b], David W. Ollila[c,i], Zibo Li[a,b]*, and Stergios J. Moschos [ID][c,d]*

[a]Departments of Radiology, The University of North Carolina at Chapel Hill (UNC-CH), Chapel Hill, NC, USA; [b]Biomedical Research Imaging Center, UNC-CH,Chapel Hill, NC, USA; [c]Lineberger Comprehensive Cancer Center, UNC-CH, Chapel Hill, NC, USA; [d]Departments of Medicine, The University of North Carolina at Chapel Hill (UNC-CH), Chapel Hill, NC, USA; [e]Departments of Pathology And Laboratory Medicine, The University of North Carolina at Chapel Hill (UNC-CH), Chapel Hill, NC, USA; [f]Departments of Dermatology, The University of North Carolina at Chapel Hill (UNC-CH), Chapel Hill, NC, USA; [g]Department of Biostatistics, The University of North Carolina Gillings School of Global Public Health, Chapel Hill, NC, USA; [h]Departments of Cell Biology and Physiology, The University of North Carolina at Chapel Hill (UNC-CH), Chapel Hill, NC, USA; [i]Departmant of Surgery, The University of North Carolina at Chapel Hill (UNC-CH), Chapel Hill, NC, USA

ABSTRACT

Clinical trials of combined IDO/PD1 blockade in metastatic melanoma (MM) failed to show additional clinical benefit compared to PD1-alone inhibition. We reasoned that a tryptophan-metabolizing pathway other than the kynurenine one is essential. We immunohistochemically stained tissues along the nevus-to-MM progression pathway for tryptophan-metabolizing enzymes (TMEs; TPH1, TPH2, TDO2, IDO1) and the tryptophan transporter, LAT1. We assessed tryptophan and glucose metabolism by performing baseline C11-labeled α-methyl tryptophan (C11-AMT) and fluorodeoxyglucose (FDG) PET imaging of tumor lesions in a prospective clinical trial of pembrolizumab in MM (clinicaltrials.gov, NCT03089606). We found higher protein expression of all TMEs and LAT1 in melanoma cells than tumor-infiltrating lymphocytes (TILs) within MM tumors ($n = 68$). Melanoma cell-specific TPH1 and LAT1 expressions were significantly anti-correlated with TIL presence in MM. High melanoma cell-specific LAT1 and low IDO1 expression were associated with worse overall survival (OS) in MM. Exploratory optimal cutpoint survival analysis of pretreatment 'high' vs. 'low' C11-AMT SUV_{max} of the hottest tumor lesion per patient revealed that the 'low' C11-AMT SUV_{max} was associated with longer progression-free survival in our clinical trial ($n = 26$). We saw no such trends with pretreatment FDG PET SUV_{max}. Treatment of melanoma cell lines with telotristat, a TPH1 inhibitor, increased IDO expression and kynurenine production in addition to suppression of serotonin production. High melanoma tryptophan metabolism is a poor predictor of pembrolizumab response and an adverse prognostic factor. Serotoninergic but not kynurenine pathway activation may be significant. Melanoma cells outcompete adjacent TILs, eventually depriving the latter of an essential amino acid.

Introduction

Poorly immunogenic tumors have a dismal prognosis. Weak antigenicity, defective antigen presentation, expression of inhibitory cytokines, and immune cell exhaustion are well-studied mechanisms of immunoregulation.[1] Other factors that may influence host immune response, such as nutrient deprivation within the tumor microenvironment, are less understood.[2,3]

Cancer cells are metabolically flexible and can thrive by utilizing various nutrients. A microenvironment deficient in important carbon sources disables immune cells from switching to an activated/anabolic state; instead, immune cells remain in a dormant/catabolic state and struggle to survive.[4] Previous histopathologic observations that cutaneous melanomas have more peritumoral than intratumoral lymphocytes[5] suggest that a tumor microenvironment with dysregulated metabolism is clinically significant. Therapeutic strategies targeting metabolism may restore metabolic balance and improve the success of immunotherapies.

L-tryptophan (Trp) is an essential amino acid in translation and protein synthesis. However, the majority (>95%) of Trp serves as a biochemical precursor of metabolites with critical physiologic roles (reviewed in[6]) in gut homeostasis, immunity, and neuronal function. Under normal physiologic conditions, 95% of the absorbed Trp is metabolized via the kynurenine pathway by the action of indolamine

2,3-dioxygenases 1 and 2 (IDO1/IDO2) and Trp 2,3-dioxy-genase (TDO2). The resultant kynurenines are biologically active metabolites involved in inflammation, immunoregulation, excitatory neurotransmission, and gut homeostasis. Dysregulation of kynurenine metabolism can lead to various conditions, such as cancer, diabetes, mood, and psychiatric disorders (reviewed in[7]).

Increased IDO1 and TDO2 expressions have been previously reported across various malignancies. In addition, increased kynurenines have broad immunoregulatory properties and can function as oncometabolites.[8] Despite promising results in early clinical studies of combined IDO1 and PD1 inhibition in metastatic melanoma (MM),[9] randomized clinical studies failed to show a more significant clinical benefit than PD1 inhibition alone.[10] Trp metabolism in melanoma may be more complex than initially thought.

Apart from the kynurenine pathway, the role of the serotonergic pathway, an alternative pathway to Trp metabolism, is less understood. Less than 5% of the absorbed Trp is metabolized via Trp hydroxylase 1 (TPH1) and TPH2 toward serotonin (5HT)/melatonin. Serotonin plays an important physiologic role as a neurotransmitter, growth factor, angiokine, and inflammatory modulator. In cancer, serotonin has growth-stimulatory, migration/invasion, progression, and angiogenic properties (reviewed in[11]). Interestingly, high expression of TPH1 across different immune cell subsets can induce an immune-tolerant state.[12] Finally, melanoma cells can express TPHs and produce serotonin/melatonin.[13]

The lack of clinical benefit from combined IDO1 and PD1 inhibition in MM, the importance of Trp in immune system functioning, and the potential for non-kynurenine pathway-specific mechanisms of resistance of PD1 inhibitors led us to investigate the protein expression of all four Trp metabolizing enzymes (TMEs) and their transporter, LAT1, in melanoma. Furthermore, we have assessed Trp metabolism in patients with PD1 inhibitor-naïve stage IIIB-IV melanoma in a prospective clinical study of pembrolizumab (LCCC1531; clinicaltrials.gov, NCT03089606). We hypothesized that metabolic dysregulation within the tumor depletes Trp via a pathway less dependent on IDO1 expression and activity. The resultant immune dysfunction via intratumoral Trp depletion may contribute to a lesser clinical benefit from PD1 inhibitors and possibly decreased overall survival (OS).

Patients and methods

The University of North Carolina at Chapel Hill (UNC-CH) Melanocyte/Melanoma cell-line Array (CLA), the Biomax Normal Skin/Benign Nevus/Primary Melanoma Tissue Microarray (TMA), and the UNC-CH 09–1737 Metastatic Melanoma TMA

We have used (a) our previously described CLA that consists of normal human melanocytes (NHM) and 38 melanoma cell lines for immunocytochemistry (ICC).[14] (b) Commercially available TMAs that contain normal skin, benign nevi, and primary melanomas (SK181 and ME1002b; US Biomax, Inc., Derwood, MD) for immunohistochemistry (IHC). (c) Our previously described TMA consists of MM tissues collected

from patients who underwent standard-of-care (SOC) surgery for stage III/IV cutaneous melanoma at UNC-CH.[14]

The LCCC1531 trial

Patients

We enrolled adult patients with biopsiable stage IIIB-IV melanoma who had not previously received PD1 inhibitors. The study was approved by UNC-CH's Institutional Review Board (IRB). Written informed consent was obtained from all patients in compliance with the IRB's regulations. **Supplementary Material** (*Patients and Methods*) describes major eligibility criteria.

Supplementary Material (*Supplementary* Figure 1) outlines the sequence and timing of key tests and procedures. Patients underwent SOC positron emission tomography (PET) scans using fluorodeoxyglucose (FDG) co-registered with computerized tomography (CT) scans of the neck, chest, abdomen, and pelvis using intravenous (IV) contrast. After investigators identified a measurable (and biopsiable) tumor lesion(s) by Response Evaluation Criteria in Solid Tumors (RECIST) v1.1 criteria, patients underwent an α-[^{11}C]-methyl-L-tryptophan (C11-AMT) PET scan of the tumor lesion(s) of interest at the UNC-CH's Biomedical Research Imaging Center. A research tumor biopsy was performed after completing the C11-AMT PET scan and before pembrolizumab initiation. Enrolled subjects were treated with pembrolizumab, 200 mg flat dose IV, administered over 30 min every 3 weeks until progression, intolerable toxicity, or completion of up to four pembrolizumab infusions.

Supplementary Material (Patients and Methods) describes details regarding the C11-AMT PET scan protocol acquisition, image analysis, and patient monitoring during and after study completion.

Mandatory Baseline (pretreatment) Tumor Tissue Biopsies

Before pembrolizumab treatment, we collected a single mandatory research biopsy from tumor tissues previously imaged by both FDG PET and C11-AMT PET from each study participant. Representative 5 μm-thick tissue sections were stained with hematoxylin and eosin (H&E) to assess for tumor content, necrosis, and density of TILs by expert pathologists (DGT, PBG).

Tissue procurement, single-color immunohistochemistry, and digital/manual pathology scoring

We immunohistochemically stained representative 5 μm-thick sections from previously described TMAs, CLAs, and the LCCC1531 trial's research biopsies with commercially available antibodies against TPH1, TPH2, TDO2, IDO1, and LAT1. Normal human tissues and commercially available normal TMAs were antibody-stained according to the organ-specific pattern for each protein (BN501a, BN126, BN117a, US Biomax, Inc. Rockville, MD). In addition, we stained LCCC1531 tissue sections for the two principal hexokinase enzyme isoforms involved in the first enzymatic glycolysis step, hexokinase (HK) 1 and HK2, and the glucose transporter 1 (GLUT1, SLC2A1). Supplementary Material (*Supplementary Table 2*) describes
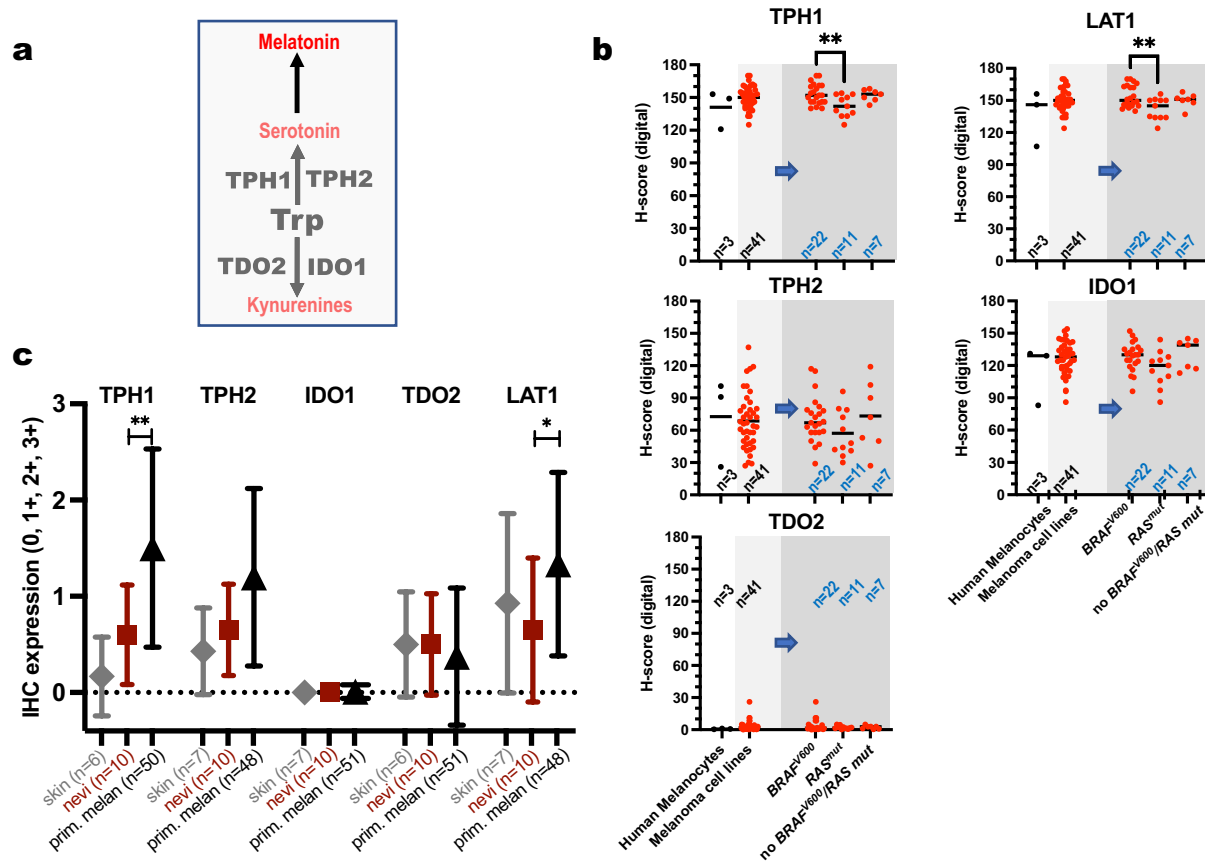
Figure 1. Protein expression of the four TMEs and LAT1 in melanoma. a. the enzymatic role of each TME is shown in the first rate-limiting enzymatic step of Trp metabolism. b. Expression (digital H-score) in NHMs (black, $n = 3$) and melanoma cell lines (red, gray boxes, $n = 41$). Within melanoma cell lines (light gray box), expression is further shown (blue arrow, dark gray region) according to the mutation status for *BRAFV600* and *RAS* mutations. c. Expression (semiquantitative 0–3 score) in normal skin ($n = 7$), nevi ($n = 10$), and primary melanomas ($n = 51$). See, Supplementary File (Patients and Methods) for histopathologic details in the analysis. Asterisks indicate significant differences in protein expression between nevi and primary melanomas. **$p < 0.01$; *$p < 0.05$.

antibodies, dilutions, and conditions for each single-color IHC assay.

The CLA and TMA slides were digitally imaged at 20× magnification using the Aperio ScanScope XT (Leica Biosystems). Images were analyzed using Aperio's Color Deconvolution Algorithm (Leica Biosystems). We presented the results as a histologic score (HScore, 0–300).[15]

Analysis of the normal skin/benign nevi/primary melanoma TMA slides (SK181, ME1002b), the metastatic melanoma 09–1737 TMAs, and the LCCC1531 tissue slides were manually performed by expert pathologists. Briefly, we semi-quantitatively analyzed TIL abundance and distribution in hematoxylin and eosin (H&E)-stained tissue sections as 0, 1 +, 2+, 3+, as we have previously described.[16] In addition, we analyzed the expression/abundance/cell distribution of the Trp and glucose metabolism-related proteins using the 0, 1 + (<25% of cells with a membrane/cytoplasmic stain), 2+ (25–80% of cells with a membrane/cytoplasmic stain), 3+ (>80% of cells with membrane/cytoplasmic stain) semiquantitative scale to describe the staining intensity and percentage of positive melanoma cells.[10] If tissue cores also included TILs, we yielded a separate 0 to 3+ score for staining intensity and percentage of positive TILs.

In Vitro studies

Details on in vitro studies are shown in Supplementary Material

Statistical analysis

Details on statistical analysis are shown in Supplementary Material.

Results

Expression of TME in NHMs, melanoma cell lines, normal skin, nevi, and primary cutaneous melanomas

We assessed the protein expression of TMEs and LAT1 in NHMs ($n = 3$), melanoma cell lines ($n = 41$), normal human skin ($n = 7$), nevi ($n = 10$), and primary melanomas ($n = 51$) by single-color ICC/IHC (Figure 1a). Supplementary Material (*Supplementary Table 3*) shows the protein expression of TMEs in NHM and melanoma cell lines. We saw no significant differences in protein expression in any of the five proteins among NHMs and all other melanoma cell lines (Figure 1b). However, among the melanoma cell lines,

TPH1 and LAT1 expressions were significantly higher in *BRAFV600*-mutant (*n* = 22) compared to *RAS*-mutant (*n* = 11) melanoma cell lines (unpaired *t*-test with Bonferroni adjusted *p*-value<0.01 for both; Figure 1b).

Figure 1c shows that the expression of TPH1, TPH2, and TDO2 was low-to-absent in normal epithelial keratinocytes and nevi. IDO1 expression was absent in normal epithelial keratinocytes, whereas the LAT1 expression was low in both. Again, compared to nevi, TPH1 and LAT1 expressionwas significantly higher in primary melanoma (Mann–Whitney test, *p* = 0.0067 and 0.0419, respectively) and did not significantly change for TPH2 and TDO2. IDO1 expression remained absent in primary melanomas.

Expression of the TMEs in stage III/IV melanoma (09–1737 cohort)

We assessed the protein expression of TMEs and LAT1 in 88 tumor tissues from 87 patients by single-color IHC. Patient characteristics are shown in Supplementary Material (*Supplementary Table 4*). In tumor cores with present TILs, expression of all five proteins was significantly higher in melanoma cells than in TILs (paired *t*-test *p*-value for all five proteins was<10^{-8}). Among the expression of the four TMEs in melanoma cells, irrespective of TIL status, IDO1 was the least expressed enzyme. In contrast, the expressions of TPH1 and TPH2 were the highest (paired *t*-test for the
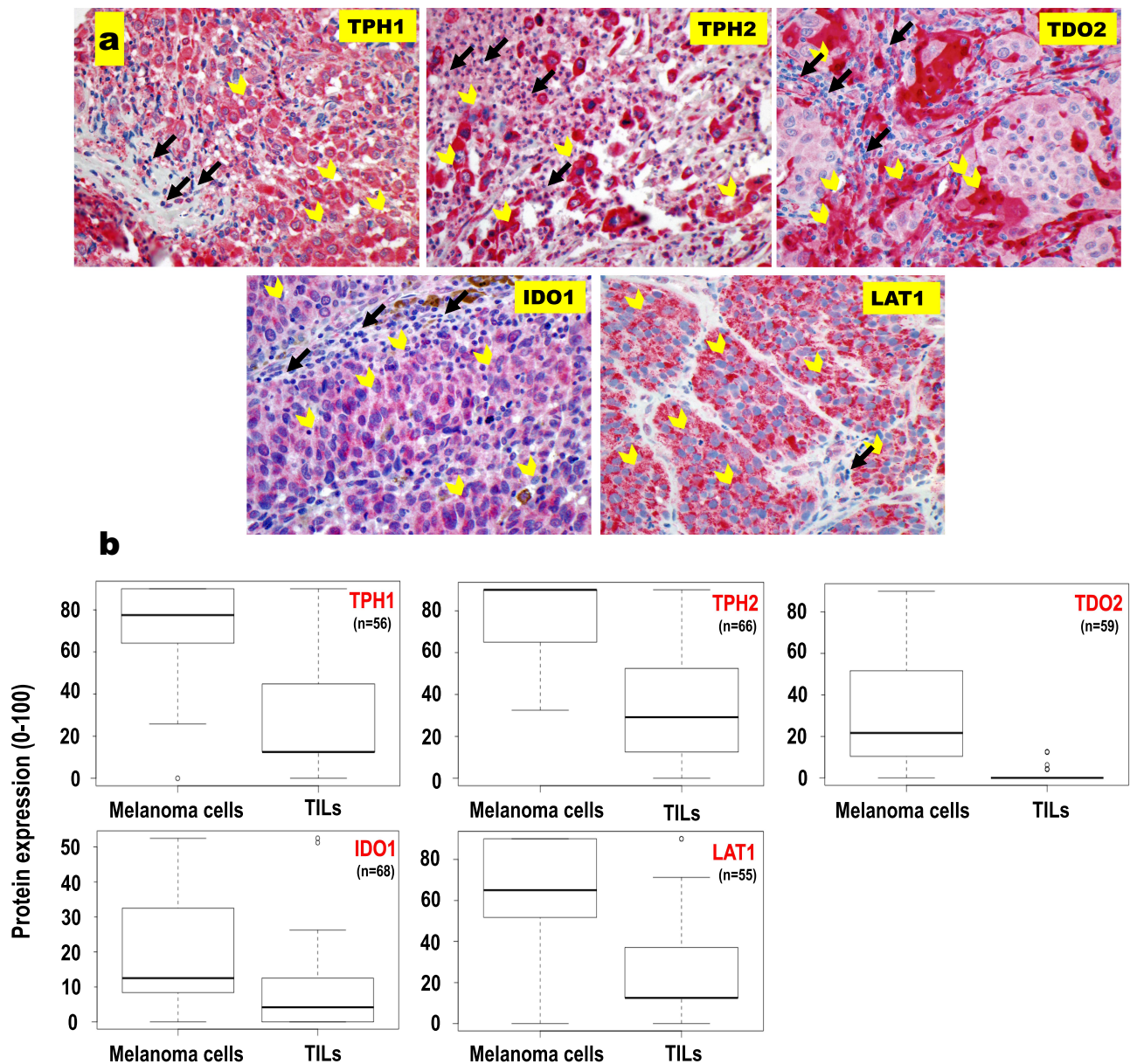
Figure 2. Expression of the TMEs and LAT1 in melanoma samples from stage III-IV melanoma patients. a. Representative images (20× magnification) were obtained from representative tumors having TILs to show differences in protein expression between melanoma cells (open yellow arrows) and TILs (black arrows). b. Boxplots show average protein expression of the proteins scored separately for melanoma cells and TILs. Only samples that had at least one value for expression of each protein in both melanoma cells and TILs for a given sample are shown.

comparison between each of TPH1, TPH2, and TDO2 enzymes with IDO1 with Bonferroni adjustment of p-value was<0.001 (Figure 2). Our results suggest that in contrast to nevi or earlier melanoma stages, protein expression of TMEs from both serotonergic and kynurenine pathways is upregulated in MM; in fact, the melanoma cell-specific expression of TPH1 and TPH2 was higher than the corresponding expression of IDO1 and TDO2. However, within tumors, melanoma cells express the four TMEs and LAT1 significantly higher than TILs.

We then hypothesized that if the expression of the TMEs and LAT1 is higher in melanoma cells than TILs, the former may overwhelmingly take up and clear Trp from the tumor microenvironment. Again, we found that increased expression of TPH1 and LAT1 in melanoma cells was significantly associated with reduced TIL presence (Supplementary Material, [*Supplementary Table 5*]). The estimated odds ratio (OR) of TIL presence compared to a sample with a one-unit higher TPH1 expression for a sample with lower TPH1 expression was 0.982 (95% confidence interval (95 CI) [0.967, 0.998], $p = 0.030$). Furthermore, the estimated OR of TIL presence for a one-unit increase in LAT1 expression was 0.984 (95 CI [0.970, 0.998], $p = 0.023$). The association tests between TIL presence and expression for the other three enzymes were inconclusive.

Prognostic significance of melanoma cell-specific protein expression of TMEs in stage III/IV melanoma (09–1737 cohort)

Given that TPH1 and LAT1 expressions in melanoma cells negatively correlats with TIL presence, we questioned whether the melanoma cell-specific expression of TMEs and LAT1 correlates with melanoma-specific OS in stage III/IV melanoma. The median follow-up of 09–1737 stage III/IV patients from tumor specimen collection was 15 months (range 1–168 months). A Cox proportional hazard model that included the average protein expression of TMEs and LAT1 and was adjusted for age, sex, and stage showed that the estimated hazard ratios (HR) for a unit increase in LAT1 and IDO1 were 1.018 (95 CI [1.004–1.032], $p = 0.016$), and 0.979 (95 CI [0.960–0.999], $p = 0.028$), respectively (Supplementary Material, [*Supplementary Table 6*]). Our results suggest that increased melanoma cell-specific expression of LAT1 is associated with a worse OS, whereas melanoma cell-specific IDO1 expression was associated with a more prolonged OS. The tests of association of TPH1, TPH2, and TDO2 expression with OS were inconclusive.

Theragnostic significance of trp and glucose in vivo `Metabolism in metastatic PD1 inhibitor-naïve melanoma (LCCC1531 study)

A higher protein expression of certain TMEs and LAT1 does not *per se* reflect higher metabolism and/or Trp uptake by the tumor. To assess Trp metabolism and uptake by patient tumors in real-time, we performed PET imaging using C11-AMT. By methylating Trp in its α-position, AMT can still be taken up by

Table 1. Patient characteristics from the LCCC1531 clinical trial ($n = 26$).

Age (yrs; median, range)	63 (30,90)
18–64	14
≥65	12
Sex (%)	
Male	20 (77)
Female	6 (33)
Melanoma Subtypes (%)	
Cutaneous	18 (69)
Acral	2 (8)
Mucosal	2 (8)
Ocular	1 (4)
Unknown Primary	3 (11)
BRAFV600E **mutation**	
Yes	3
No	15
Unknown	8
NRASQ61 **mutations**	
Yes	3
No	6
Unknown	17
AJCC staging (v7) at Original Diagnosis	
IIIB	1 (4)
IIIC	6 (23)
IIID	1 (4)
M1a	3 (11)
M1b	7 (27)
M1c	8 (31)
Prior Cancer Therapies (number of patients, %)	
No	23 (88)
Yes (adjuvant ipilimumab only)	3 (12)
ECOG Performance Status at Screening (%)	
0	19 (73)
1	7 (27)

cells via the LAT1 transporter and metabolized by all four TMEs; however, AMT can no longer participate in downstream intracellular protein synthesis steps (Supplementary Material, *Supplementary* Figure 2). We were also interested in comparing the theragnostic utility of C11-AMT PET with the 'gold standard' FDG PET.

We enrolled 26 subjects between June 2017 and November 2020 at UNC-CH who underwent C11-AMT PET, FDG PET, baseline research tumor biopsies and received at least one pembrolizumab infusion as part of the study. Table 1 shows baseline patient characteristics. The majority were males (77%) who had melanoma of cutaneous primary (69%). Sixty-nine percent of enrolled patients had AJCC stage IV melanoma. Only four patients had prior non-surgical treatment for melanoma; three had previously received adjuvant ipilimumab, and one had received talimogene laherparepvec (T-VEC).

The median duration of the pembrolizumab treatment was 5.2 months (range 0.6–34.1+ months). Supplementary Material (*Supplementary Table 7)* shows AEs that occurred in more than one study subject during the study. Figure 3 shows the swimmer's plots of all 26 patients in the study. Twenty of the 26 patients continued their care at UNC-CH after completing the 12-week study protocol; the remaining six received pembrolizumab treatment and follow-up radiographic imaging by community medical oncologists. All patients had radiographic imaging every 3 months for the first 2 years, every 6 months for the third and fourth years, and annually after that. Seven (27%) and five (19%) patients developed complete and partial radiographic responses, respectively, whereas two patients
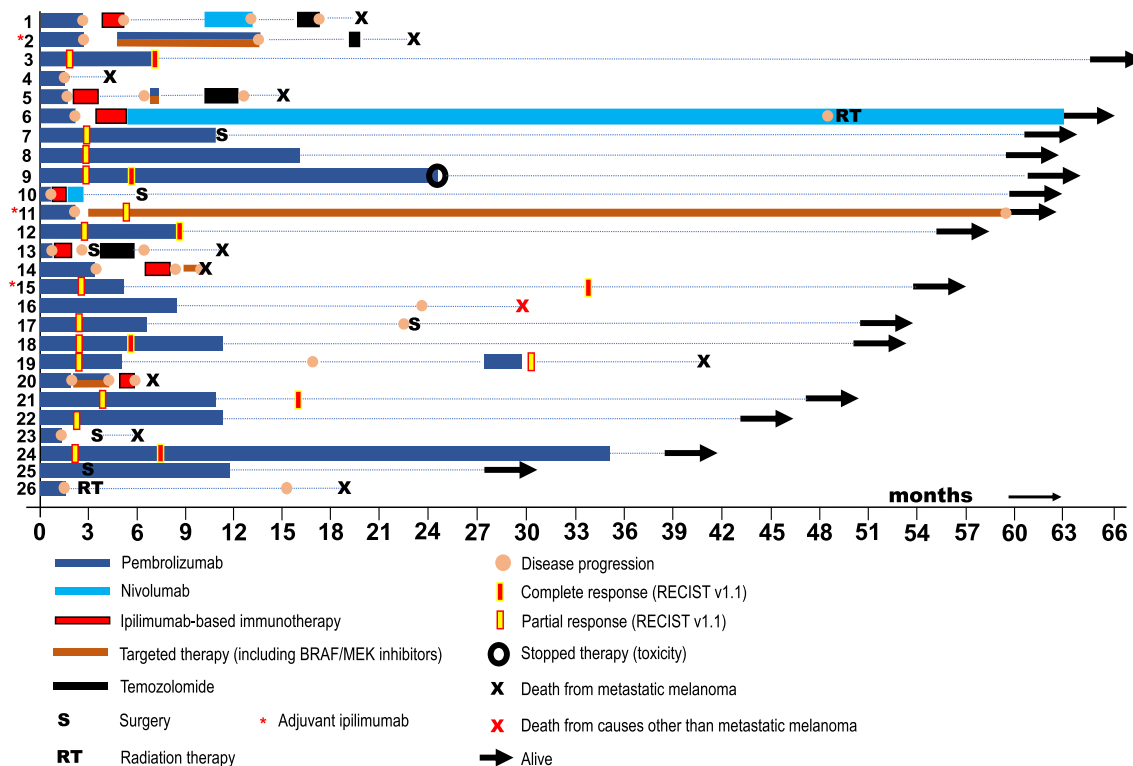
Figure 3. Swimmer's plots of patients from the LCCC1531 trial.

(8%) had stable disease as the best antitumor response (patients 16 and 24). Two of the three patients (2 and 11) who had previously received adjuvant ipilimumab had disease progression while on pembrolizumab, whereas the third patient (15) had a durable response to pembrolizumab. Two partial responders elected to undergo radical lymph node dissection (patients 7 and 25); therefore, they were censored for the PFS endpoint. Twelve patients (46%) progressed while on pembrolizumab; seven progressed before receiving four pembrolizumab infusions. The median PFS was 7.4 months (range 0.6–64.5.6+ months).

Seven of the 12 patients who progressed while on pembrolizumab received ipilimumab-based treatments; two patients had stable disease (patient 6) or partial response (patient 10) for over 3 years. One patient received BRAF/MEK inhibitor-based treatment and achieved a partial response that has endured longer than 4 years (patient 11). As of February 2023, 10 patients had died of MM. One additional patient with MM died from complications from COVID-19 infection (patient 16); he was therefore censored for the melanoma-specific OS endpoint. Six patients are alive with MM. The median OS was 42.1 months (range 4.3–64.5+ months).

Theragnostic significance of baseline trp and glucose metabolism in metastatic PD1 inhibitor-naïve melanoma (LCCC1531 study)

Sixty-one tumor lesions from all 26 patients were imaged by C11-AMT PET and FDG PET imaging and a CT scan with IV contrast before pembrolizumab treatment. The majority of imaged tumor lesions at baseline were melanoma-infiltrated lymph nodes ($n = 33$, 52%), followed by subcutaneous nodules

($n = 22$, 35%), followed by liver metastases ($n = 7$, 11%). Figure 4, panel A, shows baseline C11-AMT PET SUV_{max} values across all 61 tumor lesions for all 26 patients. The median C11-AMT SUV_{max} was 6.3 (range 1.1,23). Figure 4, panel B, shows baseline FDG PET SUV_{max} values across all 61 tumor lesions from all patients, according to tumor volume and FDG PET SUV_{max} changes following 12 weeks of pembrolizumab or earlier if progression. The median FDG SUV_{max} was 8.5 (range 2.1–22). There was a significant and moderate correlation between baseline tumor volume and SUV_{max} for both FDG and C11-AMT PET scans (Spearman rank $\rho = 0.53$, $p < 0.0001$ and $\rho = 0.45$, $p = 0.0003$, respectively). In addition, there was a significant and moderate correlation between baseline C11-AMT SUV_{max} and baseline FDG PET SUV_{max} (Spearman $\rho = 0.53$, $p < 0.0001$, Figure 4, panel C). Figure 4, panel D, shows representative images of individual tumor lesions using both PET tracers

52 out of 61 tumor lesions were also imaged with FDG PET after 12 weeks of pembrolizumab or earlier if progression. SUV_{max} increased following pembrolizumab treatment in 18 of the 20 growing tumor lesions (Wilcoxon matched-pairs signed-rank test $p = 0.0005$) and decreased following pembrolizumab treatment in 30 out of 31 shrinking tumor lesions (Wilcoxon $p < 0.0001$). In contrast, the SUV_{max} of the stable lesion increased following pembrolizumab treatment.

We performed Cox analysis to assess the value of baseline C11-AMT PET and FDG PET in predicting clinical benefit from pembrolizumab and OS. For the PFS endpoint, the estimated exponentiated coefficient for the baseline SUV_{max} of the hottest lesion per patient by C11-AMT PET imaging was 0.40 ($p = 0.07$), whereas the corresponding coefficient for FDG-PET imaging was 0.74 ($p = 0.47$).
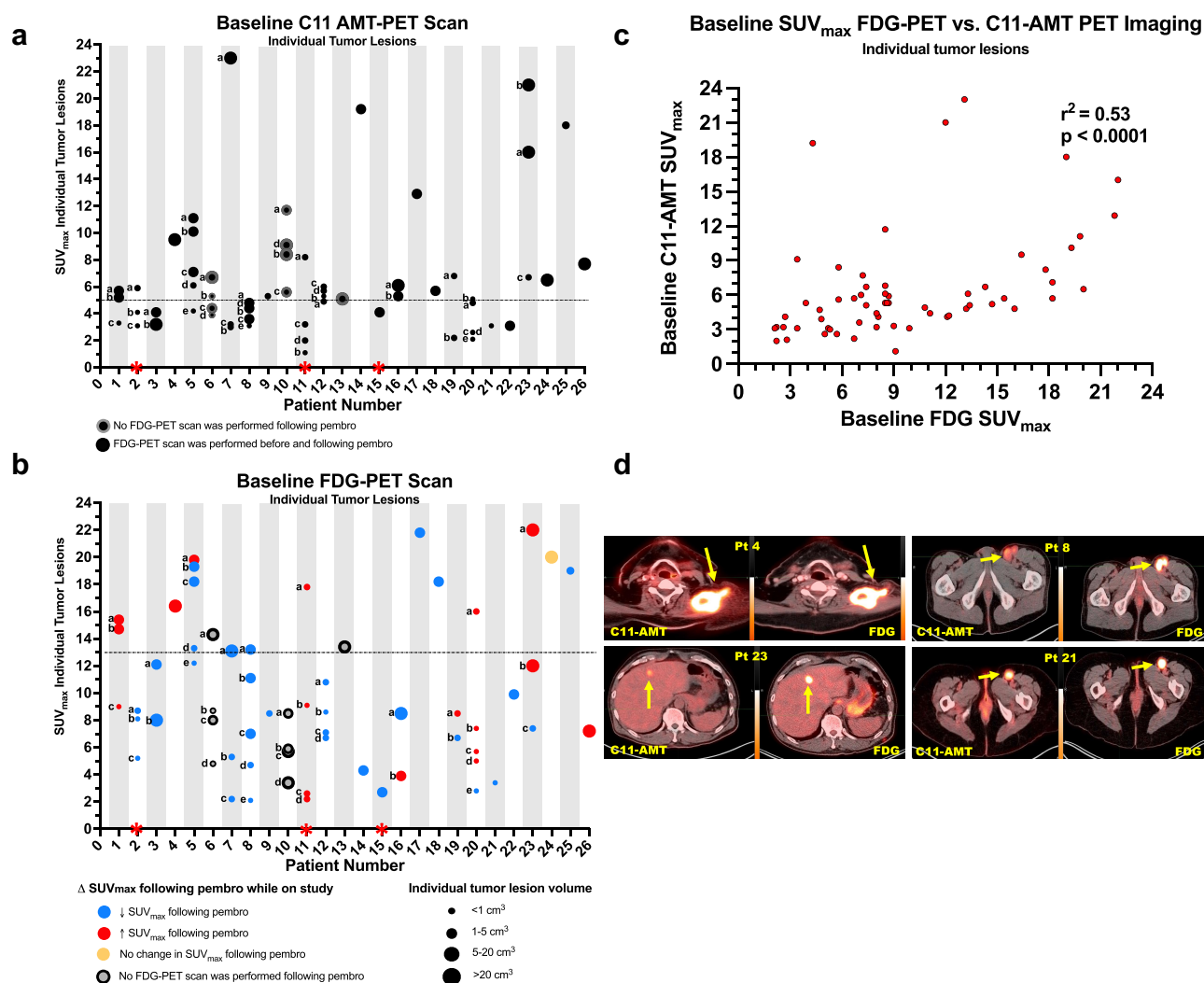
Figure 4. SUV$_{max}$ of tumor lesions imaged by C11-AMT (panel a) and FDG PET scan (panel b) prior to pembrolizumab treatment (LCCC1531 trial). SUV$_{max}$ values are shown as the ratio of the voxel with the highest radiotracer concentration compared to a 'background region' in close proximity to the tumor. Horizontal bars indicate conventional cutoff values for 'high' vs. low 'low' baseline SUV$_{max}$ (optimal cutpoint analysis, see text). Highlighted with a red asterisk are patients who had received adjuvant ipilimumab prior to study enrollment. c. Correlation between baseline SUV$_{max}$ in C11-AMT and FDG PET of tumor lesions. d. Representative images of tumor lesions from patients (pt). Each panel shows sections of the same tumor imaged with C11-AMT (left) and FDG PET scan (right). Patients 4 and 23 progressed whereas patients 8 and 21 responded to treatment.

We then performed exploratory *post-hoc* optimal cutpoint analysis of 'high' vs. 'low' SUV$_{max}$ values for baseline C11-AMT PET and FDG PET imaging. The clinical question was whether patients who remained recurrence-free while on pembrolizumab treatment or lived longer demonstrated 'higher' or 'lower' SUV$_{max}$ for C11-AMT and FDG PET prior to pembrolizumab and for a given cutpoint. By setting SUV$_{max}$ cutoff value of 5 for C11-AMT PET and 13 for FDG PET for 'high' vs. 'low' SUV$_{max}$, we found that patients with 'low' SUV$_{max}$ C11-AMT PET (one out of three patients for each of *BRAFV600E* and *NRASQ61* mutations) trended to have either stable disease, partial response, or complete response by RECIST v1.1 criteria (Fisher's exact test $p = 0.08$). However, patients with 'low' baseline SUV$_{max}$ of the hottest tumor lesion per patient by C11-AMT PET scan (two of three *BRAFV600E*-mutant and one out of three patients with *NRASQ61*-mutant) had a significantly prolonged PFS compared to patients with 'high' baseline C11-AMT PET scan [log-rank hazard ratio

(HR) 0.12, 95% confidence intervals (95 CI) 0.04–0.35, $p = 0.0128$]. 'low' baseline SUV$_{max}$ FDG PET scan only trended to prolong PFS (log-rank HR 0.44, 95 CI 0.15–1.23, $p = 0.097$. Figure 5).

Correlative analysis of baseline tumor tissue in metastatic PD1 inhibitor-naïve melanoma (LCCC1531 study)

Eighteen of the 26 mandatory research baseline tumor biopsies had a sufficient amount of viable melanoma. Fortunately, six of the eight patients whose research biopsies did not have viable melanoma had archived metastatic tumor specimens collected prior to study enrollment from previous SOC surgical procedures. Thus, 18 patients who had tumors imaged by both FDG-PET and C11-AMT PET also had subsequent research tumor biopsies with viable melanoma; these tumors were available for the correlation analysis between melanoma-specific IDO expression and baseline SUV$_{max}$ parameters. Twenty-four

Baseline C11-AMT PET Imaging

Baseline FDG PET Imaging
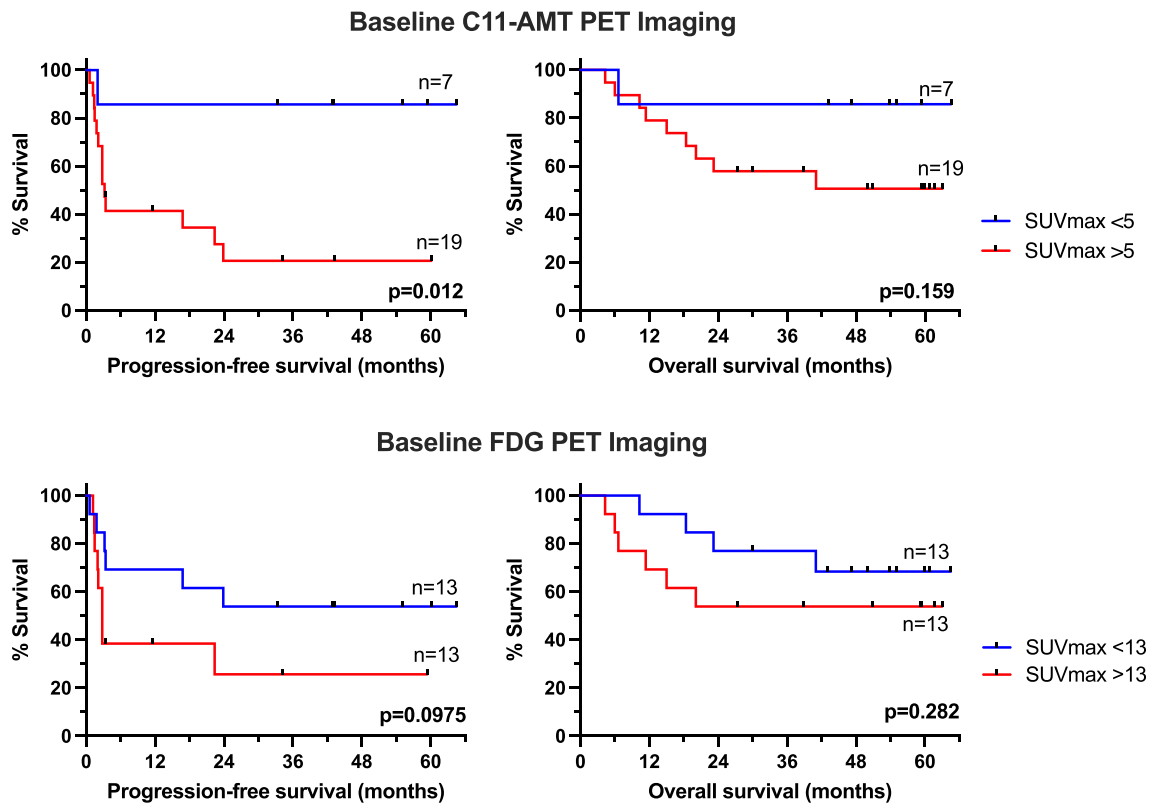
Figure 5. Theragnostic significance of baseline SUV$_{max}$ using C11-AMT PET and FDG PET imaging in metastatic PD1 inhibitor-naive melanoma using optimal cutpoint post-hoc analysis. the hottest tumor lesion from each patient was only included in the analysis.

pretreatment tumor specimens (archived plus research) were available for other tumor tissue correlative analyses.

We found that high expression of IDO1 by melanoma cells trended to correlate with low C11-AMT SUV$_{max}$ values of these tumors (Kendall τ rank correlation −0.34, $p = 0.08$) but not with TIL density based on H&E stains (Kendall τ = 0.17, $p = 0.37$). We found no significant correlation between IDO1 expression and FDG PET SUV$_{max}$ values (−0.20, $p = 0.30$). In addition, there were no significant differences in either PFS or OS among patients bearing tumors with high (2+, 3+) vs. absent/low (0, 1+) TILs by H&E analysis (data not shown). If present, we then compared the protein expression for each protein involved in the Trp and glucose metabolism between melanoma cells and TILs. After adjusting the critical p-value for multiple comparisons using the Bonferroni correction ($p = 0.0064$), TPH1, TDO2, LAT1, and HK2 expression by melanoma cells was significantly higher than the corresponding expression by TILs (Supplementary Material, *Supplementary Figure 3*). The expression (high vs. low/absent) of none of the proteins involved in Trp and glucose metabolism was associated with PFS, OS, baseline FDG PET SUV$_{max}$, and baseline C11-AMT PET SUV$_{max}$ of the hottest tumor lesion per patient. Finally, we correlated the expression of LAT1 with GLUT1 in melanoma cells and TILs, since cellular uptake of metabolites significantly contributes to pathway activity, among other factors (e.g., abundance and activity of each rate-limiting enzymatic component within the given pathway). We found no correlation between LAT1 and GLUT1 expression in melanoma cells (Kendall τ=-0.05, $p = 0.82$) and TILs (Kendall τ = 0.11, $p = 0.85$).

Nine patients had available *BRAFV600mut/NRASmut* status (three *BRAFV600mut*, two *NRASmut*, and four wild-type *for BRAFV600/NRASmut*). All three *BRAFV600mut* tumors had strong (3+) TPH1/LAT1 expression in melanoma cells, whereas only two out of four *BRAFV600/NRAS*-wild type tumors and one out of two *NRASmut* tumors had strong (3+) expression of both TPH1/LAT1.

Finally, we explored the correlation among the proteins involved in Trp, glucose metabolism, and TILs. Among the highest significant correlations were seen between TPH1 and LAT1 expression by melanoma and TILs (Spearman rank correlation coefficient ρ=+0.81 and+0.83, respectively; $p < 0.0001$ and 0.003, respectively), between HK1 expression in TILs and TIL density (ρ = 0.81, $p = 0.004$) and between TDO2 expression in melanoma cells and TIL density (ρ = 0.62, $p = 0.003$).

Treatment of melanoma cell lines with telotristat

The high expression of TPH1 in primary and MM, its higher expression by melanoma cells compared to neighboring TILs, and the reduced abundance of TILs in melanomas bearing a high expression of TPH1 prompted us to investigate the effect of pharmacologic inhibition of TPH1 in melanoma cell lines *in vitro*. Treatment of SK-MEL-2 and MeWo cell lines with increasing concentrations of telotristat etiprate, a TPH1 inhibitor, for 72 hours did not significantly affect cell growth or cell death. However, telotristat treatment significantly increased IDO protein expression in melanoma cells, whereas TPH1 expression remained relatively unaltered. Furthermore, the
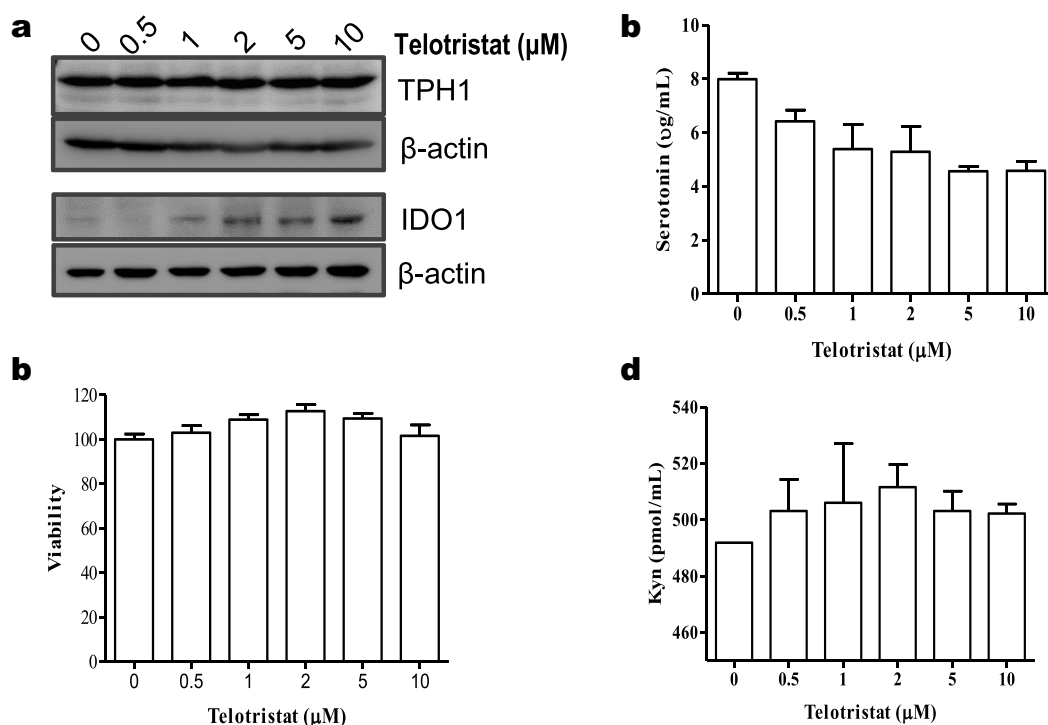
Figure 6. Treatment of SK-MEL-2 melanoma cells with telotristat. a. Immunoblot analysis of cell lysates 24 hours post treatment initiation. Experiment was performed in triplicates. b. Cell viability using a MTT assay 72 hours following treatment initiation. Experiment was performed in duplicates. c & d. ELISPOT assay for serotonin and kynurenine (Kyn) 24 hours following post treatment initiation. Experiment was performed in duplicates.

effects of telotristat on TPH1 and IDO1 expression in melanoma cells were associated with significant changes in serotonin (reduced) and kynurenine (increased) levels cell-line culture medium (Figure 6). These results may highlight metabolic flexibility in melanoma cells, such that pharmacologic inhibition of the serotonin pathway may lead to a compensatory increase in the kynurenine pathway in melanoma cells.

Discussion

This study shows that MM exhibits dysregulation in Trp metabolism, similar to other solid tumors.[17,18] Despite the study limitations (overall small patient number in the LCCC1531 study and a disproportionate number of patients with cutaneous metastases and primary cutaneous melanoma), this is the first report that directly compares a Trp-like PET tracer, such as C11-AMT, with FDG, the gold standard diagnostic PET tracer in oncology, within the same patient in this prospective intervention study. Baseline FDG PET imaging only trended to prolong PFS in patients who receive single-agent pembrolizumab in stage III/IV melanoma using a *post-hoc* optimal cutpoint exploratory survival analysis, as we have previously described.[19,20] Despite the lack of statistical significance, perhaps partly due to the small patient number, this statistical trend is in line with other reports from more extensive prospective studies in oncology, which showed the theragnostic significance of FDG PET imaging across various solid tumors.[21,22] Nevertheless, our study is the first to report that high Trp imaging trended to associate with shorter clinical benefit from pembrolizumab in PD1 inhibitor-naïve MM OS

in a Cox analysis and significantly prolonged PFS using the optimal cutpoint exploratory survival analysis.

How can the metabolism of an amino acid such as Trp have a better predictive role in clinical benefit from pembrolizumab but not glucose? Trp is an essential amino acid for mammalian cells and vital for anabolic processes in melanoma and immune cells.[6] In fact, intratumoral Trp levels rise many times higher than in the plasma via various mechanisms (reviewed in[23]). Our IHC analysis across MM samples shows that the expression of all TMEs and LAT1 is significantly higher in melanoma cells than in TILs. We hypothesize that, melanoma cells have a greater capacity for uptake and metabolism of Trp within this competitive tumor microenvironment than adjacent TILs. Higher Trp uptake and metabolism within melanoma cells have two adverse outcomes for TILs. First, Trp depletion eventually deprives lymphocytes of an amino acid necessary for proliferation.[24] Disabled immune cells are thus forced to switch from an activated/anabolic state to a dormant/catabolic state and struggle to survive.[4] Second, Trp metabolism within melanoma cells produces kynurenines and serotonin that exert an immunoregulatory function on TILs.[25,26] In contrast, glucose is not only available through diet, but can be produced intracellularly via several other intracellular pathways. Although glucose uptake and metabolism can be higher in tumor cells than TILs and may lead to defects in T cell effector function, other metabolic pathways (e.g., glutamine, fatty acids, cholesterol) can partially compensate for defective glucose metabolism within T-cells (reviewed in[27]).

We noticed a significant positive correlation between SUV_{max} in baseline C11-AMT and FDG PET imaging for individual tumor lesions from the LCCC1531 study. Given the significant correlation of each SUV_{max} with individual

tumor volumes, we must assume that in vivo metabolism for both Trp and glucose is principally driven by melanoma cells. Nevertheless, only approximately 50% of the SUV_{max} variability value in C11-AMT could be predicted by the SUV_{max} in FDG PET, suggesting that a nonspecific rev-up of global tumor metabolism in melanoma cells cannot solely explain our findings. In line with this, we did not find any correlation between LAT1 and GLUT1 expression in melanoma cells or TILs, suggesting that at least cellular uptake of each metabolite, which is one of the three crucial components of metabolic pathway activity, is regulated by different mechanisms. More specifically, we were surprised to find low-to-moderate expression levels of GLUT1 in both melanoma cells and TILs, contrasting the consistently high levels of LAT1 in both cell populations. The redundancy of glucose transport may alternatively explain this discrepancy via other glucose transporters we did not measure in this study. Alternatively, we postulate that while Trp is an essential nutrient for any cell, normal or malignant, glucose is not because glucose can be produced via different intracellular metabolic pathways, especially by the metabolically more flexible melanoma cells. Besides, we have previously shown that glycolysis is not melanoma cells' principal metabolic pathway.[28]

Given the lack of higher clinical benefit from combined IDO1 and PD1 inhibition in MM,[10] we sought to better understand the relative contribution of the kynurenine and serotonin/melatonin pathway in the overall Trp metabolism within tumors, given that C11-AMT is not specific for one pathway over the other. We, therefore, performed an extensive IHC analysis of cell lines and tissue specimens across all stages of the nevus-melanoma progression pathway for TMEs and LAT1. To our surprise, we identified increased TPH1 and LAT1 along the nevus-melanoma progression pathway, whereas the expression of TDO2 and IDO1 was relatively unchanged. Although upregulation of an enzyme(s) does not automatically correspond to a higher enzymatic activity, our finding that TPH1 and LAT1 were significantly higher in *BRAFV600*-mutant as opposed to *RAS*-mutant melanoma cell lines suggests that oncogenic mutations such as *BRAFV600E*, may, among other mechanisms, contribute to the metabolic reprogramming of melanoma cells by selectively upregulating serotonin/melatonin but not kynurenines. Due to small patient numbers in the LCCC1531 study with complete information about the *BRAFV600E* and *NRAS* mutation status, we have been unable to validate these *in vitro* findings in our prospective study. In addition, in our clinical study, C11-AMT SUV_{max} of the biopsied lesion trended to anti-correlate with melanoma-specific IDO1 expression, again suggesting that the high C11-AMT SUV_{max} signal could possibly be driven by non-IDO1-associated Trp metabolizing pathways. In support of the importance of the serotoninergic pathway, a recent metabolomic analysis of sera collected from patients with IIIC/IV MM and sex-/age-matched controls showed not only significant alterations in Trp metabolism in MM but also higher serum serotonin, but not kynurenine, levels.[29] Finally, a single remote case report showed increased intratumoral levels of serotonin in melanoma tumors.[30] These results suggest that upregulation of the serotonin/melatonin but not the

kynurenine pathway may account for the higher Trp metabolism in melanoma cells.

We have herein shown that low baseline C11-AMT PET scan SUV_{max} of the hottest tumor from the LCCC1531 patients is associated with a prolonged OS in a post hoc optimal cut-point exploratory survival analysis; this is in line with our findings from a multivariate analysis of prognostic factors from the 09–1737 patient cohort, which showed that high LAT1 expression by melanoma cells is an adverse prognostic factor. Interestingly, high expression of IDO1 by melanoma cells was a favorable prognostic factor in the 09–1737 patient cohort, perhaps because IDO1 is upregulated in response to a pro-inflammatory environment (IFNγ, TNFα). The latter signifies the poorly characterized (pro-tumorigenic vs. antitumor) role of serotonin/melatonin in cancer.[11]

Telotristat is the first FDA-approved TPH1 inhibitor for patients with carcinoid syndrome.[31] Interestingly, in syngeneic colorectal and pancreatic tumors, telotristat augmented effects of PD-1 checkpoint blockade and increased tumor-infiltrating CD8+ cells by suppressing serotonin-mediated upregulation of PD-L1 in tumor cells.[25] We found that telotristat suppressed serotonin production by melanoma cells without significant effects in melanoma cell proliferation. Interestingly, however, telotristat increased expression of IDO1 in melanoma cell lines, which may account for the increased kynurenine concentrations in cell-line supernatants. Given the compensatory changes within the kynurenine pathway in response to telotristat treatment in melanoma cell lines, future *in vivo* studies investigating the potential for reversing PD1 inhibitor resistance by concurrent treatment with telotristat ± IDO1 inhibition in syngeneic melanoma mouse models are being considered.

Our results have important clinical implications. First, the predictive significance of *in vivo* Trp imaging in patients treated with pembrolizumab at least in MM may justify the development of F^{18}-based Trp PET probes for broader clinical use, in particular to predict the response to PD1 inhibitors, given C11-AMT's very short half-life. Such probes can be further designed to be 'agnostic' or pathway-nonspecific (i.e., serotonin/melatonin vs. kynurenine), given that different cancers may preferentially metabolize Trp toward one pathway and not the other.[32] In fact, we have recently developed a series of F^{18}-F-5-OMed-Trp PET probes that are more IDO1-specific, show excellent tumor uptake in melanoma-bearing syngeneic models,[33] and can be used in future clinical trials for precise immunotherapy monitoring. Lastly, given the availability of TPH1 inhibitors in the clinic, targeting TPH1 in patients with PD1 inhibitor-refractory melanoma may potentially restore PD1 inhibitor resistance.

Abbreviations

Trp, tryptophan; IDO1, indoleamine 2,3-dioxygenase; TDO2, tryptophan 2,3-dioxygenase-2; MM, metastatic melanoma; TPH, tryptophan hydroxylase; TMEs, tryptophan-metabolizing enzymes; LAT1/SLC7A5, Large neutral amino acid transporter small subunit-1; TILs, tumor-infiltrating lymphocytes; OS, overall survival; CLA, cell-line array; ICC, immunocytochemistry; TMA, tissue microarray; IHC, immunohistochemistry; SOC, standard of care; UNC-CH, University of North Carolina at Chapel Hill;

PET, positron emission photography; FDG, fluorodeoxyglucose; CT, computerized tomography; IV, intravenous; RECIST, OR, odds ratio; 95 CI, 95% confidence intervals.

Acknowledgments

Disclosure statement

Funding

ORCID

Stergios J. Moschos http://orcid.org/0000-0002-8943-0845

Data availability statement

The data that support the findings of this study are available from the corresponding author, SJM, upon reasonable request.

References

1. Blankenstein T, Coulie PG, Gilboa E, Jaffee EM. The determinants of tumour immunogenicity. Nat Rev Cancer. 2012;12(4):307–313. doi:10.1038/nrc3246. PMID: 22378190.
2. Singer K, Cheng W-C, Kreutz M, Ho P-C, Siska PJ. Immunometabolism in cancer at a glance. Dis Model Mech. 2018;11(8). dmm034272. doi:10.1242/dmm.034272.
3. Kedia-Mehta N, Finlay DK. Competition for nutrients and its role in controlling immune responses. Nat Commun. 2019;10(1):2123. doi:10.1038/s41467-019-10015-4.
4. Wang A, Luan HH, Medzhitov R. An evolutionary perspective on immunometabolism. Science. 2019;363(6423):eaar3932. doi:10.1126/science.aar3932.
5. Erdag G, Schaefer JT, Smolkin ME, Deacon DH, Shea SM, Dengel LT, Patterson JW, Slingluff CL Jr. Immunotype and immunohistologic characteristics of tumor-infiltrating immune cells are associated with clinical outcome in metastatic melanoma. Cancer Res. 2012;72(5):1070–1080. [Epub 2012 Jan 19]. http://doi.org/10.1158/0008-5472.CAN-11-3218.
6. Perez-Castro L, Garcia R, Venkateswaran N, Barnes S, Conacci-Sorrell M. Tryptophan and its metabolites in normal physiology and cancer etiology. FEBS J. 2023;290(1):7–27. [Epub 2021 Nov 7]. doi:10.1111/febs.16245.
7. Cervenka I, Agudelo LZ, Ruas JL. Kynurenines: tryptophan's metabolites in exercise, inflammation, and mental health. Science. 2017;357(6349):eaaf9794. doi:10.1126/science.aaf9794.
8. Uyttenhove C, Pilotte L, Theate I, Stroobant V, Colau D, Parmentier N, Boon T, Van den Eynde BJ. Evidence for a tumoral immune resistance mechanism based on tryptophan degradation by indoleamine 2,3-dioxygenase. Nat Med. 2003;9 (10):1269–1274. [Epub 2003 Sep 21]. doi:10.1038/nm934.
9. Mitchell TC, Hamid O, Smith DC, Bauer TM, Wasser JS, Olszanski AJ, Luke JJ, Balmanoukian AS, Schmidt EV, Zhao Y, et al. Epacadostat plus pembrolizumab in patients with advanced solid tumors: phase I results from a multicenter, open-label phase I/

II trial (ECHO-202/KEYNOTE-037). J Clin Oncol. 2018;36 (32):3223–3230. [Epub 2018 Sep 28]. doi:10.1200/JCO.2018.78.9602.
10. Long GV, Dummer R, Hamid O, Gajewski TF, Caglevic C, Dalle S, Arance A, Carlino MS, Grob JJ, Kim TM, et al. Epacadostat plus pembrolizumab versus placebo plus pembrolizumab in patients with unresectable or metastatic melanoma (ECHO-301/KEYNOTE-252): a phase 3, randomised, double-blind study. Lancet Oncol. 2019;20(8):1083–1097. [Epub 2019 Jun 17]. doi:10.1016/S1470-2045(19)30274-8.
11. Sarrouilhe D, Mesnil M. Serotonin and human cancer: a critical view. Biochimie. 2019;161:46–50. [Epub 2018 Jun 21]. doi:10.1016/j.biochi.2018.06.016.
12. Nowak EC, de Vries VC, Wasiuk A, Ahonen C, Bennett KA, Le Mercier I, Ha DG, Noelle RJ. Tryptophan hydroxylase-1 regulates immune tolerance and inflammation. J Exp Med. 2012;209 (11):2127–3235. doi:10.1084/jem.20120408.
13. Slominski A, Semak I, Pisarchik A, Sweatman T, Szczesniewski A, Wortsman J. Conversion of L-tryptophan to serotonin and melatonin in human melanoma cells. FEBS Lett. 2002;511(1–3):102–106. doi:10.1016/s0014-5793(01)03319-1.
14. Carson CC, Moschos SJ, Edmiston SN, Darr DB, Nikolaishvili-Feinberg N, Groben PA, Zhou X, Kuan PF, Pandey S, Chan KT, et al. IL2 Inducible T-cell kinase, a novel therapeutic target in melanoma. Clin Cancer Res. 2015;21(9):2167–2176. doi:10.1158/1078-0432.CCR-14-1826.
15. Rizzardi AE, Johnson AT, Vogel RI, Pambuccian SE, Henriksen J, Skubitz AP, Metzger GJ, Schmechel SC. Quantitative comparison of immunohistochemical staining measured by digital image analysis versus pathologist visual scoring. Diagn Pathol. 2012;7(1):42. doi:10.1186/1746-1596-7-42.
16. Googe PB, Theocharis S, Pergaris A, Li H, Yan Y, McKenna EF Jr, Moschos SJ. Theragnostic significance of tumor-infiltrating lymphocytes and Ki67 in BRAFV600-mutant metastatic melanoma (BRIM-3 trial). Curr Probl Cancer. 2022;46(3):100862. [Epub 2022 Apr 2]. doi:10.1016/j.currproblcancer.2022.100862.
17. Juhasz C, Nahleh Z, Zitron I, Chugani DC, Janabi MZ, Bandyopadhyay S, Ali-Fehmi R, Mangner TJ, Chakraborty PK, Mittal S, et al. Tryptophan metabolism in breast cancers: molecular imaging and immunohistochemistry studies. Nucl Med Biol. 2012;39(7):926–932. [Epub 2012 Mar 22]. doi:10.1016/j.nucmedbio.2012.01.010.
18. Batista CE, Juhasz C, Muzik O, Kupsky WJ, Barger G, Chugani HT, Mittal S, Sood S, Chakraborty PK, Chugani DC. Imaging correlates of differential expression of indoleamine 2,3-dioxygenase in human brain tumors. Mol Imaging Biol. 2009;11(6):460–466. [Epub May 12]. doi:10.1007/s11307-009-0225-0.
19. Moschos SJ, Eroglu Z, NI NI, Kendra KL, Ansstas G, In GK, Wang P, Liu G, Collichio FA, Googe PB, et al. Targeting the IL-2 inducible kinase in melanoma; a phase 2 study of ibrutinib in systemic treatment-refractory distant metastatic cutaneous melanoma: preclinical rationale, biology, and clinical activity (NCI9922). Melanoma Res. 2021;31(2):162–172. doi:10.1097/CMR.0000000000000726.
20. Trembath DG, Davis ES, Rao S, Bradler E, Saada AF, Midkiff BR, Snavely AC, Ewend MG, Collichio FA, Lee CB, et al. Brain tumor microenvironment and angiogenesis in melanoma brain metastases. Front Oncol. 2020;10:604213. eCollection 2020. doi:10.3389/fonc.2020.604213.
21. Costelloe CM, Macapinlac HA, Madewell JE, Fitzgerald NE, Mawlawi OR, Rohren EM, Raymond AK, Lewis VO, Anderson PM, Bassett RL, et al. 18F-FDG PET/CT as an indicator of progression-free and overall survival in osteosarcoma. J Nucl Med. 2009;50(3):340–347. doi:10.2967/jnumed.108.058461.
22. Zhao K, Wang C, Shi F, Huang Y, Ma L, Li M, Song Y. Combined prognostic value of the SUVmax derived from FDG-PET and the lymphocyte-monocyte ratio in patients with stage IIIB-IV non-small cell lung cancer receiving chemotherapy. BMC Cancer. 2021;21(1):66. doi:10.1186/s12885-021-07784-x.

23. Badawy AAB. Targeting tryptophan availability to tumors: the answer to immune escape? Immunol Cell Biol. 2018;96 (10):1026–1034. [Epub 2018 Jun 10]. doi:10.1111/imcb.12168.

24. Munn DH, Shafizadeh E, Attwood JT, Bondarev I, Pashine A, Mellor AL. Inhibition of T cell proliferation by macrophage tryptophan catabolism. J Exp Med. 1999;189(9):1363–1372. doi:10.1084/jem.189.9.1363.

25. Schneider MA, Heeb L, Beffinger MM, Pantelyushin S, Linecker M, Roth L, Lehmann K, Ungethum U, Kobold S, Graf R, et al. Attenuation of peripheral serotonin inhibits tumor growth and enhances immune checkpoint blockade therapy in murine tumor models. Sci Transl Med. 2021;13(611):eabc8188. doi:10.1126/scitranslmed.abc8188.

26. van Baren N, Van den Eynde BJ. Tryptophan-degrading enzymes in tumoral immune resistance. Front Immunol. 2015;6:34. eCollection 2015. doi:10.3389/fimmu.2015.00034.

27. Chapman NM, Chi H. Metabolic adaptation of lymphocytes in immunity and disease. Immunity. 2022;55(1):14–30. doi:10.1016/j.immuni.2021.12.012.

28. Ho J, de Moura MB, Lin Y, Bateman NW, Hood BL, Sun M, Suhan J, Duensing S, Yin Y, Sander C, et al. Importance of glycolysis and oxidative phosphorylation in advanced melanoma. Mol Cancer. 2012;11(1):76. doi:10.1186/1476-4598-11-76.

29. Bayci AWL, Baker DA, Somerset AE, Turkoglu O, Hothem Z, Callahan RE, Mandal R, Han B, Bjorndahl T, Wishart D, et al. Metabolomic identification of diagnostic serum-based biomarkers for advanced stage melanoma. Metabolomics. 2018;14(18):105. doi:10.1007/s11306-018-1398-9.

30. Horai T, Nishihara H, Hattori S, Tateishi R. Malignant melanoma producing serotonin. Cancer. 1979;43(1):294–298. doi:10.1002/1097-0142(197901)43:1<294:aid-cncr2820430142>3.0.co;2-v.

31. Kulke MH, Horsch D, Caplin ME, Anthony LB, Bergsland E, Oberg K, Welin S, Warner RR, Lombard-Bohas C, Kunz PL, et al. Telotristat ethyl, a tryptophan hydroxylase inhibitor for the treatment of carcinoid syndrome. J Clin Oncol. 2017;35 (1):14–23. [Epub 2016 Oct 28]. doi:10.1200/JCO.2016.69.2780.

32. Giglio BC, Fei H, Wang M, Wang H, He L, Feng H, Wu Z, Lu H, Li Z. Synthesis of 5-[(18)F]Fluoro-alpha-methyl tryptophan: new trp based PET agents. Theranostics. 2017;7(6):1524–1530. eCollection 2017. doi:10.7150/thno.19371.

33. Wu X, Ma X, Zhong Y, Chen W, Xu M, Zhang H, Wang L, Tu X, Han Z, Zhao W, et al. Development of [18F]F-5-OMe-tryptophans through photoredox radiofluorination: a new method to access tryptophan-based PET agents. J Med Chem. 2023 Feb 24;66(5):3262–3272. Online ahead of print. doi:10.1021/acs.jmedchem.2c01544.